

## COMBUSTION OF UNSUPPORTED METHANOL/DODECANOL MIXTURE DROPLETS AT LOW GRAVITY

J. C. YANG, G. S. JACKSON AND C. T. AVEDISIAN  
*Sibley School of Mechanical and Aerospace Engineering  
Cornell University  
Ithaca, New York 14853*

Experiments are reported on the combustion of free or unsupported methanol/dodecanol mixture droplets in a reduced gravity environment. The experiments were conducted in a drop tower. The Grashof number (based on drop diameter) in the moving frame of reference was on the order of  $10^{-5}$  for the period of droplet burning.

Combustion of the mixture droplets was characterized by a multi-stage process indicative of diffusion controlled burning. The flame was not visible during the first stage because of the lighting used, but was visible (and spherical) in the final stage. The results suggested that the mixture droplets did not extinguish. By contrast, methanol droplets consistently extinguished. Microexplosions were not observed for mixtures with initial concentrations of equal volumes of methanol and dodecanol. However, most of the droplets containing initially 75% (by volume) of methanol exploded. The initiation of microexplosion, as defined by the occurrence of homogeneous nucleation within the droplet, is explained by comparing the calculated nonlinear variation of superheat limit with composition for a methanol/dodecanol mixture with the boiling point of dodecanol.

### Introduction

This paper reports the results of an experimental study of the burning of free or unsupported non-sooting fuel droplets in a low gravity environment. The low gravity environment, created by the use of a drop tower,<sup>1</sup> minimizes axial vapor flows around a burning droplet. The data obtained from burning under such conditions can be compared to analyses which assume spherically symmetric combustion.

Pure methanol droplets and mixture droplets of methanol and 1-dodecanol were burned in the present study. Alcohols produce little or no soot relative to other combustible liquids which makes data obtained from them advantageous for comparing with theoretical models because the presence of soot introduces analytical complications, such as its effect on heat transfer to the droplet. Furthermore, the physical properties of alcohol mixtures, such as the limit of superheat,<sup>2</sup> can be readily calculated using existing analyses, and thus, predictions, like the potential for microexplosion, can be made concerning the combustion process.

A primary motivation for studying methanol/dodecanol mixtures is that the large volatility difference between the two liquids creates the potential for microexplosions. Also, mixtures of liquids with a large volatility differential offer an opportunity for examining preferential vaporization characteristics. The absence of an axial vapor flow around the

droplet, created by a low gravity environment and minimal movement of the droplet during combustion, can allow for these preferential vaporization phenomena to be observed without effects of internal circulation in the droplet, which can occur during burning at normal gravity because of buoyancy.

The following liquids were studied: pure methanol, mixtures containing initially 50% (by volume) methanol in dodecanol (corresponding to a methanol mole fraction of .85) and mixtures with 75% (by volume) methanol with dodecanol (corresponding to a methanol mole fraction of .94). The equal volume mixture was selected because prior experiments carried out under earth normal gravity have shown that monodispersed droplet streams of this composition exhibited enhanced microexplosion characteristics.<sup>3</sup> The 75% mixture was studied because of considerations involving the superheat limit of the mixture and the boiling point of dodecanol as discussed in Section 3.

Both a low gravity environment and small initial drop sizes provided for low buoyancy conditions. Initial droplet diameters ranged from 400  $\mu\text{m}$  to 600  $\mu\text{m}$ . The current drop package<sup>1</sup> achieves gravity levels on the order of  $10^{-3}$  earth normal gravity. Gravity level or droplet diameter alone, however, does not govern the extent to which buoyancy-induced flows may be neglected. Rather, the Grashof number provides a measure of the importance of

buoyancy; gravity, droplet diameter, ambient pressure, and ambient temperature collectively contribute to the importance of buoyancy induced flows.<sup>4</sup> In the present work, the Grashof number based on droplet diameter remained less than  $3 \times 10^{-5}$  over the droplet burning period. Such a low value renders valid the neglect of buoyancy as demonstrated by the spherically symmetric flame shapes observed around the droplets in the present study. Lower Grashof numbers, which can be attained by the use of a drag shield around the instrumentation package to further reduce gravity levels, were not deemed necessary.

A motivation for studying small droplets is that most practical combustion situations employ small droplets, usually on the order of 100  $\mu\text{m}$  or less (e.g., burning sprays).<sup>5</sup> Also, a study of small unsupported droplets is complementary to other low gravity droplet studies that have employed larger droplets, on the order of 1 mm initial diameter.<sup>6,7,8</sup> The effects of initial droplet size are not yet fully understood.

An unsupported droplet at low gravity was created by propelling the droplet upward in a near vertical trajectory within the combustion chamber and then releasing the package with the chamber and on-board instrumentation into free-fall when the droplet reached the apex of its trajectory. The method reported in prior studies<sup>1,4,9</sup> was modified in the present work by 1) igniting the droplets after the free-fall began, 2) using two electrode pairs symmetrically placed around the droplet and 3) retracting the electrodes after ignition. The first two modifications were made in an attempt to address concerns about spherically symmetric conditions around the droplet at ignition. The electrodes were retracted to prevent them from acting as a heat sink for the flame. In the present study, the far ambience around the droplet was room temperature air at .101 MPa.

## Experiment

### Description of the Apparatus:

The drop package on which the experiment takes place contains the droplet generator, a high speed movie camera, a video camera, combustion chamber, spark ignition system, and the lighting unit. Detailed descriptions of the components of the drop tower facility and experimental apparatus are described elsewhere.<sup>1,4,9</sup> Some recent modifications are described below.

A 75 mm f/1.4 camera lens with an extension tube was attached to the high speed camera to photograph the test droplet. Camera framing rates between 200 frames/s and 400 frames/s were used. The film was Kodak TRI-X reversal ASA 200 film.

Backlighting was provided by a 13VAC halogen projector lamp with a diffuser, and the voltage supplied to the lamp was varied depending on the luminosity of the flame. A CCD video camera was mounted on the drop package to facilitate adjusting the droplet trajectory prior to initiating an experimental run. The high gain of light intensity on the CCD camera provided qualitative pictures of the flames around the burning droplets.

Figure 1 is a schematic diagram of the droplet generator together with the electrode mount system, which is partially described in the introduction. The four electrodes were hung from a support plate with guide rails and held in place by the pin of a solenoid. The electrodes were withdrawn by two springs after retraction of the solenoid pin. The electrode retraction mechanism was mounted to a three-dimensional translation stage. Droplet generation, package release, spark activation, and electrode retraction were coordinated by a timing control circuit as in previous work.<sup>1,4,9</sup>

### Data Reduction:

Droplet diameters were measured from the motion picture sequences by a frame-by-frame analysis of the movies. A film projector was mounted 65 cm vertically above a drafting board on which the droplet image was projected. Maximum vertical ( $D_v$ ) and horizontal ( $D_h$ ) dimensions of the image were marked. A scale factor was obtained from the image of a ball bearing (3.97 mm diameter). An equivalent droplet diameter ( $D_{eq}$ ) was then calculated by assuming that the droplet was a sphere having a volume equal to that of an ellipsoid with  $D_h$  and  $D_v$  as its major and minor axes, respectively.

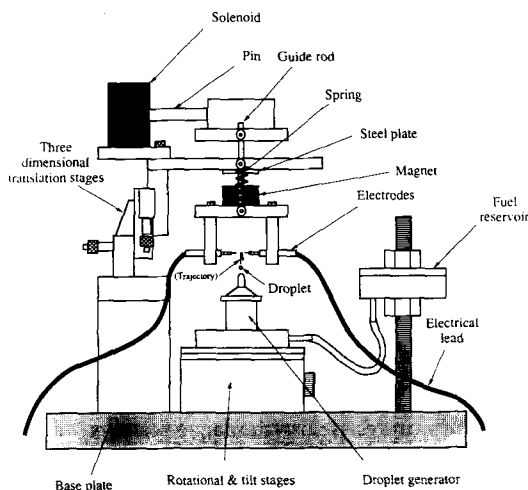


FIG. 1. Schematic of the electrode configuration with retraction mechanism.

The above method of data reduction has a measure of uncertainty of about  $10\ \mu\text{m}$ . This uncertainty is about 2% of the initial droplet diameters in this study, but for droplet diameters of  $50\ \mu\text{m}$  or less, the uncertainty becomes too large a percentage to provide accurate measurements. However, droplets with diameters much less than  $50\ \mu\text{m}$  can still be observed with the optical set-up.

Measurements for two runs from the above method were compared with those made from a commercially available frame-grabbing system, the Olympus™ CUE-2 Image Analysis System. The data analyses showed agreement between diameters measured from the two methods to within 5% over the entire range of observation.

### Results and Discussion

The evolutions of droplet diameter for pure methanol and for 50/50 and 75/25 methanol/dodecanol mixtures are shown in Figs. 2 to 4. Seven experimental runs of pure methanol shown in Fig. 2 demonstrate the extent of repeatability of the

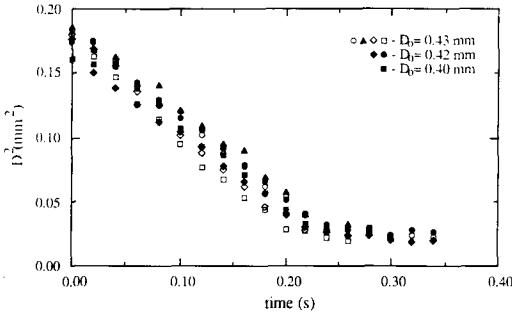


FIG. 2. Evolution of diameter squared for methanol droplets burning at low gravity.

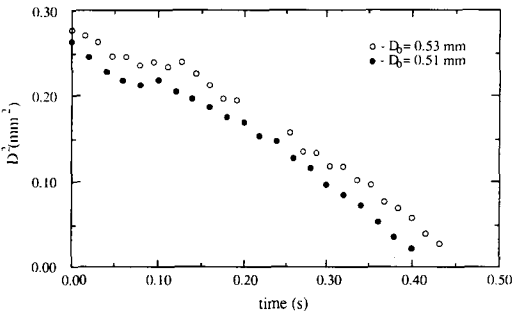


FIG. 3. Evolution of diameter squared for two 50/50 methanol/dodecanol droplets burning at low gravity.

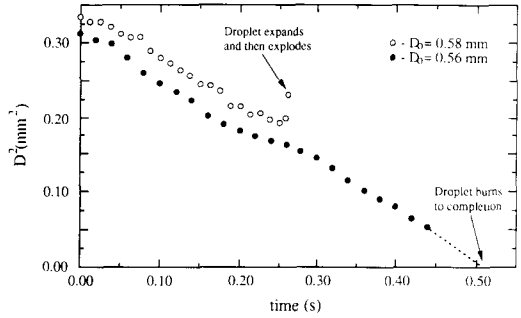


FIG. 4. Evolution of diameter squared for two 75/25 methanol/dodecanol droplets burning at low gravity.

measurements. The initial diameters ranged from .40 mm to .43 mm. The differences in initial diameters, though small, can account for the spread in the curves shown in Fig. 2.

Representative photographic sequences of a methanol droplet and methanol/dodecanol mixture droplets are shown in Fig. 5. The different background shading for the run in Fig. 5b was used because the flame was luminous enough to be recorded for the latter stage of burning with the 50/50 mixture runs. The flame, however, could only be recorded on the film with the dimmer backlighting. The apparent dumbbell shape of the droplet at  $t = 0\text{s}$  was produced by the reflection of the two sparks on opposite sides of the droplet. The electrodes are visible only at  $t = 0\text{s}$  after which they were retracted. Measurements of the evolution of flame diameter are not reported because the photographic reproductions of the flame images, though spherical and visible, were too faint to get accurate diameter measurements.

The evolution of droplet diameter is presented in the form suggested by the classical quasi-steady spherically symmetric "D<sup>2</sup>" law for droplet combustion,<sup>10</sup>

$$D^2 = D_0^2 - Kt \quad (1)$$

where  $D$  is the droplet diameter,  $D_0$  is the initial droplet diameter,  $t$  is time and  $K$  is the so-called burning rate constant

$$K = -d(D^2)/dt \quad (2)$$

Equations 1 and 2 may provide predictions of the diameter evolution provided that the physical properties are properly selected to evaluate  $K$ . However, these choices for property values are rather ad-hoc, and the classical "D<sup>2</sup>" law can not account for flame extinction. Because extinction of the pure methanol droplets was observed in the present study,

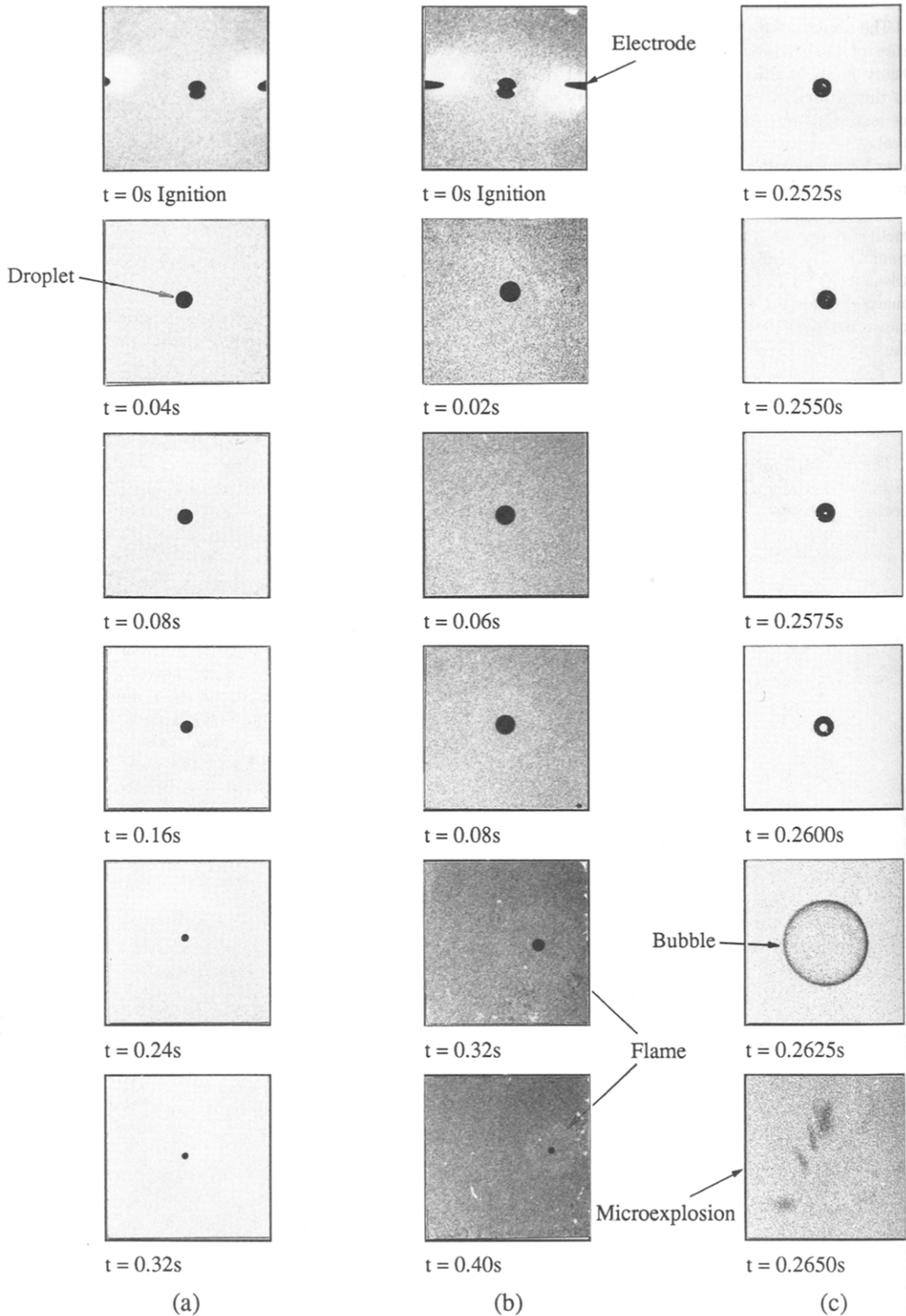


FIG. 5. Photographic sequences of burning droplets: (a) pure methanol -  $D_o = 0.43$  mm, (b) 50% dodecanol/50% methanol by volume -  $D_o = 0.51$  mm, (c) 75% methanol/25% dodecanol showing microexplosions -  $D_o = 0.58$  mm. Different enlargement was used in (c).

no predictions were made concerning burning rate constants. In the present study, only general trends are noted.

The data for pure methanol droplets shown in Fig. 2 seem to indicate that a unique burning rate can characterize the diameter evolution for the first 0.2 s of burning. The evidence, though, is not conclusive that the burning rate does not vary with time. Another study has reported variations with time in the burning rate for methanol droplets burning in an oxygen/helium environment.<sup>8</sup> Variations in the burning rate constant of methanol have been discussed based on water vapor produced by the combustion being absorbed by the droplet. In the present study, any possible curvature in the evolution of diameter to reveal such a mechanism for variations in  $K$  could not be definitively distinguished.

Near the end of burning of the pure methanol droplets, the droplet diameter appeared to reach a constant value (*cf.* Fig. 5a). This fact indicates extinction of the flame around the droplet.<sup>6,9</sup> Extinction was observed in all of the methanol droplets studied, and this agrees with observations in the combustion of larger single component free alcohol (methanol and ethanol) droplets burning in a low gravity environment.<sup>6,8</sup> Extinction diameters ( $D_e$ ) measured in the present study ranged from .16 mm to .19 mm (the average value was about .17 mm). The seven data sets shown in Fig. 2 may appear to be suggestive of a unique extinction diameter. However, this small variance in  $D_e$  may have been due to the small range of  $D_o$  for the runs, and hence, no definitive value can be quoted as a universal extinction diameter for methanol burning in air.

Three observations to note in regard to the burning of the mixture droplets are the following: 1) droplet burning apparently consisted of a three-stage process for both mixture compositions studied, 2) extinction did not occur for the mixtures, and 3) microexplosions were not observed for the equi-volume mixture but were observed for the 75/25 mixture as discussed below.

Three-stage combustion is characterized by a plateau region in the evolution of droplet diameter (*cf.*  $t \sim .1$  s for the 50/50 mixture in Fig. 3 and to a lesser extent at  $t \sim .26$  s for the 75/25 mixture in Fig. 4). Three-stage combustion could be indicative of distillation or diffusion-controlled vaporization mechanism.<sup>3</sup> In distillation-controlled vaporization, the mixture components will vaporize in the order of their relative volatilities and the instantaneous droplet concentration will be uniform. Diffusion-controlled burning is characterized by preferential vaporization initially of the more volatile species, which results in an increase in the concentration of the less volatile species near the droplet surface. Because of liquid diffusional resistance, the more volatile species gradually becomes depleted at the droplet surface and cannot be replenished fast

enough to allow for its complete vaporization. This results in concentration gradients within the droplet.

Two observations suggest a predominantly diffusion-controlled mechanism as characterizing the combustion process. Firstly, the volume reduction of the droplet by the second-stage of burning (e.g.,  $\sim 25\%$  for the 50/50 mixture runs) can not account for complete removal of the methanol, and this implies that in the final stage of combustion both dodecanol and methanol are vaporized. Such simultaneous vaporization of both components is explained by a diffusion-controlled mechanism. Secondly, the occurrence of microexplosion implies concentration gradients within the liquid phase which can only be explained by a diffusion-controlled mechanism.

Since methanol vaporization will dominate in the early period of combustion (before the relatively flat region in Figs. 3 and 4), the flame image during this early period should be less visible than in the final stage when both methanol and dodecanol are vaporizing simultaneously. The photographic prints shown in Fig. 5a show that the flame is not visible around the methanol droplet with the optical set-up used for the high speed movie camera. It was also not distinctly visible with the more light-sensitive video camera. Hence, the inability to record the flame with either camera during the early stage of combustion for the methanol/dodecanol mixtures may indicate that almost pure methanol is being vaporized during this period.

For  $t > .1$  s with the 50/50 mixture burning, the spherical flame becomes faintly visible around the droplet as shown in Fig. 5b ( $t = .32$  s and .4 s). The flame should be expected to be more luminous in the final stage than in the first because dodecanol plays a more pronounced role in vaporization during the final stage. Long carbon chain species in the gas phase surrounding the droplet resulting from the dodecanol vaporization could promote soot formation and thereby yield a more luminous flame.

Microexplosions did not occur in the present study for 50/50 mixture droplets burning at low gravity. However, they have been observed for this mixture in experiments on monodispersed burning droplet streams at earth normal gravity.<sup>3</sup> Results from these prior experiments reported that microexplosions for the 50/50 mixtures occurred when the droplet reached a size such that  $D/D_o \approx .42$ . Figure 3 shows that the droplets survived to smaller diameters (to  $D/D_o \approx .3$ ), and the movie record indicated that the droplets continued to shrink until vanishing completely. Thus, it seems reasonable to assume that microexplosions did not occur for these droplets.

On the other hand, microexplosions were observed for the 75/25 mixture droplets studied, although a few droplets of this mixture did not mi-

croexplode. Microexplosions were characterized by a bubble forming within the droplet, then growing to expand the droplet, and finally bursting as shown in Fig. 5c. These results are explained with reference to Fig. 6.

The superheat limit of a methanol/dodecanol mixture is shown as a function of composition. The calculation was performed with the aid of a relatively accurate method for predicting the superheat limit of a mixture based on corresponding states principle. The method is described elsewhere.<sup>2</sup> A volume fraction average critical temperature was taken for the mixture.<sup>11</sup> The variation of superheat limit with mixture composition is nonlinear. If

$$T_d(x_i, P) > T_s(x_i, P), \quad (3)$$

where  $T_s$  and  $T_d$  are the superheat limit and droplet burning temperature, respectively, then microexplosions may be initiated.

$T_d$  cannot exceed the dodecanol boiling point during the droplet lifetime: it can only be approached as methanol is progressively depleted from the droplet during vaporization. Using, then, an assumption that the droplet does reach the boiling point of dodecanol and that the composition in the interior of the droplet is the initial composition at the start of burning, Fig. 6 shows that  $T_d > T_s$  for  $x_{\text{methanol}} > x_i = .85$  (initial molar concentration of the 50/50 by volume mixture). Thus, microexplosions should not occur for the 50/50 mixture but may be expected to occur for the 75/25 mixture where initial molar concentration ( $x_i = .94$ ) provides a  $T_s$  below the assumed maximum  $T_d$ . This prediction is supported by the majority of the present experimental results for the 75/25 mixture droplets.

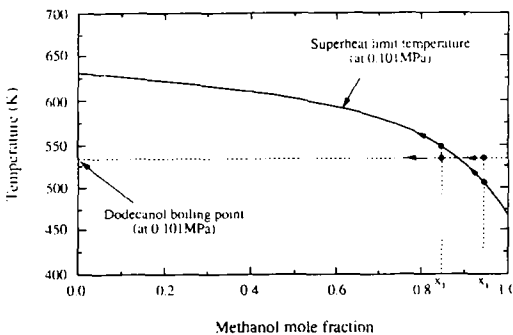


FIG. 6. Comparison of the calculated variation of superheat limit of a methanol/dodecanol mixture with composition. The horizontal line is the boiling point (at .101 MPa) of dodecanol and the vertical lines indicate initial mole fractions of methanol for the mixtures studied. Arrows indicate the direction of change of droplet composition during burning.

However, microexplosions were not observed in all of the 75/25 mixture droplets studied. The 75/25 composition is near the threshold defined by eq. 3 where  $T_s$  equals the maximum possible  $T_d$  (boiling point of dodecanol) as shown in Fig. 6. Because the droplet will be progressively depleted of methanol as burning proceeds, the  $T_s$  of the local mixture concentrations within the droplet will tend to rise as the concentration of methanol is decreased.

Increase in local  $T_s$  will be most prominent near the surface of the droplet where methanol is depleted more rapidly. When the methanol is depleted near the surface, the  $T_d$  will also rise. If the local  $T_s$  near the surface increases above  $T_d$ , then microexplosion may only occur if the heating at the surface can diffuse into the droplet interior where methanol concentrations are still near the initial mixture composition and the local  $T_s$  is still below  $T_d$ . In such a case, the occurrence of microexplosion will be dependent upon whether the heating of the droplet interior will be fast enough to occur before diffusion of methanol to the surface causes a rise in the interior  $T_s$  such that eq. 3 can not be satisfied. However, if  $T_d$  increases above the local  $T_s$  near the surface, microexplosion can be initiated in this region. As the 75/25 mixture of methanol/dodecanol has an initial  $T_s$  near the maximum possible  $T_d$ , it is highly possible that for this mixture the rise in local  $T_s$  due to methanol depletion will sometimes suppress microexplosion.

Slight variations in the experimental conditions affecting combustion may cause the time variation of  $T_s$  and/or  $T_d$  for the 75/25 mixture droplets to change enough such that microexplosion sometimes will and sometimes will not occur. Any of the following may have slightly changed between experimental runs: the extent of initial internal circulation within the droplet at ignition, the disturbance of the spark, variations in the initial droplet diameter or droplet velocity, etc. . . . The effects of small changes in these conditions on liquid phase temperature and concentration profiles are difficult to quantify. This may account for observing five runs of the 75/25 mixture droplets which did not microexplode and thirteen runs which did.

The plateau region which characterizes the second stage of combustion was less pronounced for the few 75/25 mixture droplets which did not microexplode as shown in Fig. 4. Microexplosions took place at about the same time after ignition as the second-stage of burning (as indicated by the visibility of the flame on the video record) occurred for the droplets which did not microexplode.

The observation of complete burning for all the 50/50 mixtures and some 75/25 mixtures of methanol and dodecanol show that the addition of dodecanol can suppress extinction observed in pure methanol droplets. This result may suggest a less pronounced effect of water vapor absorption in the

methanol/dodecanol mixture droplets than in pure methanol droplets. If the droplet surface is rich in dodecanol during the third stage of the three stage combustion process, water absorption within the droplet may be insignificant during combustion because of the lower solubility of water in dodecanol than methanol. Furthermore, the surface temperature of the droplet should be high enough to suppress water condensation on the surface.

### Conclusions

This experimental study of low gravity spherically symmetric combustion of unsupported methanol/dodecanol mixture droplets has revealed preferential vaporization. The experimental observations suggest that methanol dominates vaporization during an initial period, followed by a period in which dodecanol begins to vaporize significantly. The spherical flame was visible in the final stage but not the first. This visibility was conjectured to be promoted by the presence of dodecanol and its intermediate species in the gas phase which, with their carbon chains, may form soot precursors and hence, result in a more luminous flame.

Microexplosions were observed for a 75% volume mixture of methanol but not for a 50% volume mixture. This fact was explained based on comparing the dodecanol boiling point with the superheat limit of the mixture. Methanol droplets consistently experienced extinction, while the mixture droplets studied did not, which suggests that the mixing of a heavy alcohol with methanol may help to suppress extinction of pure methanol droplets.

### Acknowledgments

This work was supported by the National Aeronautics and Space Administration (Grant No. NAG 3-987), the National Science Foundation (Grant No.

CBT-8451075), and the New York State Center for Hazardous Waste Management.

### REFERENCES

1. AVEDISIAN, C. T., YANG, J. C. AND WANG, C. H.: Proc. Roy. Soc. Lond. A420, 183 (1988).
2. AVEDISIAN, C. T. AND SULLIVAN, J. R.: Chem. Eng. Sci. 39, 1033 (1984).
3. WANG, C. H. AND LAW, C. K.: Comb. Flame 59, 53 (1985).
4. YANG, J. C., JACKSON, G. S. AND AVEDISIAN, C. T., AIP Conference Proceedings 197: Drops and Bubbles, American Institute of Physics, p. 394, 1989.
5. PRESSER, C., GUPTA, A. K., SEMERJIAN, H. G. AND SANTORO, R. J.: Proc. ASME/JSME Thermal Eng. Joint Conf., Vol. 1, 73, Honolulu, March 22-27, 1987.
6. HARA, H. AND KUMAGAI, S.: presented at the 12th. Int. Colloquium on Dynamics of Explosions and Reactive Systems, University of Michigan, Ann Arbor, July 23-28, 1989.
7. CHOI, M. Y., DRYER, F. L., Haggard, J. B. AND BRACE, M.: AIP Conference Proceedings 197: Drops and Bubbles, Am. Inst. of Physics, p. 338, 1989.
8. CHOI, M. Y., CHO, S. Y., DRYER, F. L. AND HAGGARD, J. B.: Paper No. 73, Eastern States Section Meeting, The Combustion Institute, Albany, NY, October 30, 31, November 1, 1989.
9. YANG, J. C. AND AVEDISIAN, C. T.: Twenty-Second Symposium (International) on Combustion, p. 2037, The Combustion Institute, 1989.
10. SPALDING, D. B.: Fourth Symposium (International) on Combustion, p. 847, The Combustion Institute, 1953.
11. REID, R. C., PRAUSNITZ, J. M., AND POLING, B. E.: Properties of Gases of Liquids, 4th ed., New York, McGraw Hill, 1987.